Experimental investigation on the effect of heterogeneous hull roughness on ship resistance

Soonseok Song [a,*], Roberto Ravenna [a], Saishuai Dai [a], Claire DeMarco Muscat-Fenech [b], Giorgio Tani [c], Yigit Kemal Demirel [a], Mehmet Atlar [a], Sandy Day [a], Atilla Incecik [a]

[a] Department of Naval Architecture, Ocean and Marine Engineering, University of Strathclyde, 100 Montrose Street, Glasgow, UK
[b] Faculty of Engineering, University of Malta, Msida, MSD2080, Malta
[c] Department of Electrical, Electronic, Telecommunication Engineering and Naval Architecture, Università degli Studi di Genova, Italy

ARTICLE INFO

ABSTRACT

There has been an increasing attention to the effect of hull roughness on ship resistance and powering. In conventional studies, the hull surfaces have been treated as uniform rough surfaces while the real ships' hulls are exposed heterogeneous fouling accumulation. The work described here presents an experimental investigation into the effect of heterogeneous hull roughness on ship resistance. A series of towing tests were conducted using a ship model of the Wigley hull with various hull roughness conditions, including homogeneous conditions (i.e. smooth and full-rough conditions) and heterogeneous conditions (i.e. ¼-bow-rough, ¼-aft-rough, ½-bow-rough and ½-aft-rough conditions). The bow-rough conditions (e.g. ¼-bow-rough and ½-bow-rough) showed larger added resistance than aft-rough conditions (e.g. ¼-aft-rough and ½-aft-rough) with the same wetted surface area of the rough region. This finding suggests that the hull roughness of the forward part of the hull is more significant than the others in terms of the added resistance. Finally, a new method was proposed to predict the added resistance due to the heterogeneous hull roughness based on Granville's similarity law scaling and the predictions were compared with the experimental result.

1. Introduction

One of the main reasons for the performance degradation of ships is increased hull roughness. The hull roughness of a ship increases by time due to various factors, such as corrosion and biofouling (Tezdogan and Demirel, 2014; Townsin, 2003). The ship resistance increases markedly with increased hull roughness and thus economic and environmental penalties follow. Accordingly, there has been extensive research carried out in order to predict the effect of hull roughness on ship resistance and powering, either using the similarity law scaling or Computational Fluid Dynamics (CFD).

The similarity law scaling method of Granville (1958; 1978) has been the most popular method to predict the roughness effect on ship resistance (e.g. Schultz, 2002; Schultz, 2004; Schultz and Flack, 2007; Flack and Schultz, 2010; Schultz et al., 2011; Demirel et al., 2017a; Demirel et al., 2019; Li et al., 2019; Uzun et al., 2019; 2020). The advantages of using the Granville's method include that it can predict the roughness effect on the skin friction of a flat plate of arbitrary length and speeds,

once the roughness function of the surface is known. This flat plate assumption is generally considered as reasonable and it shows good agreement with other high-fidelity methods (Demirel et al., 2017b; Song et al., 2019a) while it requires much less computational cost. Recently, Song et al. (2020a) validated this method by comparing the predicted result with the experimental data involving a towed ship model with a rough surface.

During the past few years, there has been increasing attention to modelling the roughness effect using CFD simulations. One of the merits of using CFD is that the three-dimensional (3D) effects can be taken into account, which makes it possible to predict the roughness effect on the pressure-related ship resistance components as well as the effect on the propeller performance. A recent trend is using modified wall-functions by employing the roughness function of the given rough surface into the simulation models (e.g. Demirel et al., 2014; Demirel et al., 2017b; Farkas et al., 2018; Song et al., 2019a; Song et al., 2019b; Song et al., 2020b; Song et al., 2020c; Song et al., 2020d; Farkas et al., 2020). Recently, Song et al. (2020e) validated the similarity law scaling and the
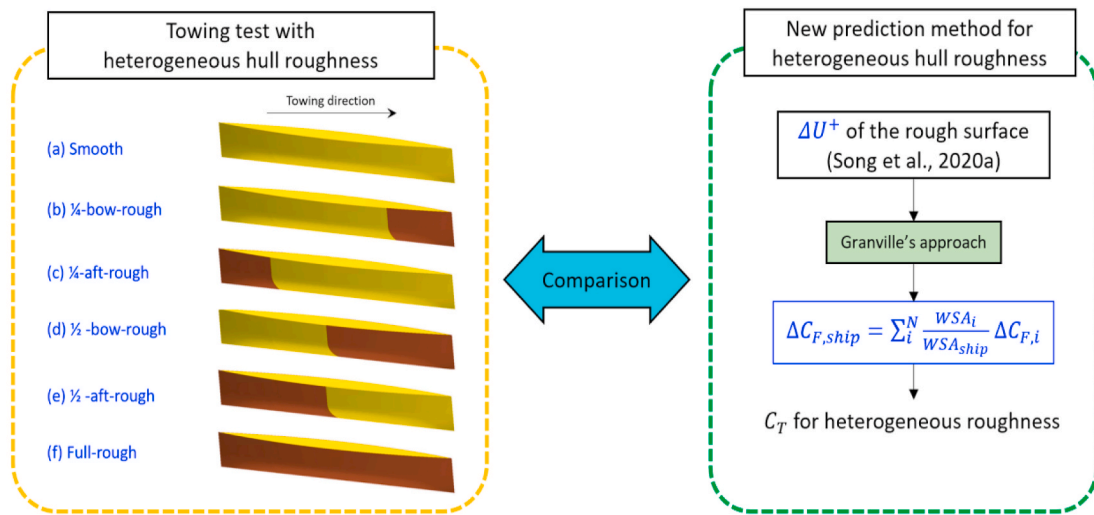
Figure 1 Schematic illustration of the current methodology

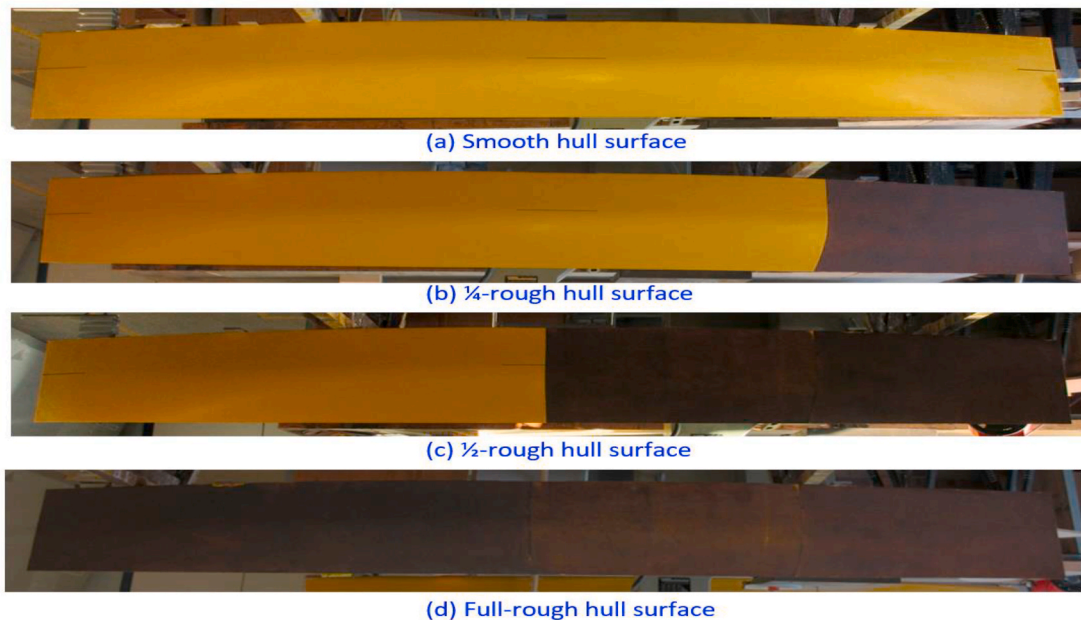**Fig. 1.** Schematic illustration of the current methodology.

Fig. 2. Wigley model with different surface conditions.

CFD approach by comparing the predictions with the towing tests involving a ship model with a rough surface.

However, in the above studies, the hull surfaces have been treated as uniformly rough, while the real ships' surfaces are not uniform due to the exposition to heterogeneous fouling accumulation. This difference can introduce uncertainties in the added resistance predictions, as claimed by Demirel et al. (2017a). Furthermore, Pullin et al. (2017) asserted that the roughness effect varies with the downstream distance. This implies that the hull roughness in the different regions may have different contributions to the added resistance. Therefore, it is worthwhile to investigate whether the heterogeneous distribution of hull roughness brings different results compared to the case of homogeneous hull roughness (i.e. evenly distributed hull roughness).

To the best of the authors' knowledge, there exists no specific study investigating the effect of heterogeneous distributions of hull roughness

on ship resistance. Therefore, this study aims to fill this gap by conducting towing tests of a ship model with heterogeneous hull roughness.

In this study, towing tests were conducted using a Wigley hull model with heterogeneous hull roughness conditions (i.e. ¼-bow-rough, ¼-aft-rough, ½-bow-rough and ½-aft-rough conditions) as well as homogeneous conditions (i.e. smooth and full-rough conditions), by applying sand grit on the hull surface systematically. A new prediction method was proposed to predict the added resistance due to the heterogeneous hull roughness and the predictions were compared with the experimental result.

Fig. 3. The towing carriage of the Kelvin Hydrodynamics Laboratory and the Wigley model; (a)½-bow-rough condition, (b) ½-aft-rough condition.

Table 1
Principal particulars of the Wigley model and test conditions.

Length	L (m)	3.00
Beam at waterline	B (m)	0.30
Draft	T (m)	0.1875
Beam/draft ratio	B/T	1.6
Total wetted surface area	WSA (m^2)	1.3383
Wetted surface area of first quarter	WSA_{Q1} (m^2)	0.3066
Wetted surface area of first half	WSA_{H1} (m^2)	0.6691
Displacement	∇ (m^3)	0.0750
Block coefficient	C_B	0.4444
Towing speed	V (m/s)	1.08–2.71
Froude number	Fn	0.2–0.5
Reynolds number	Re_L	2.6–6.6 × 10^6
Water temperature	T_w (°C)	12

2. Methodology

2.1. Approach

Fig. 1 schematically illustrates the methodology used in this study. A series of towing tests of the Wigley hull model were conducted with different hull conditions including the heterogeneous hull conditions (i. e. ¼-bow-rough, ¼-aft-rough, ½-bow-rough and ½-aft-rough conditions) as well as the homogeneous hull conditions (i.e. smooth and full-rough conditions). In order to roughen the hull surface heterogeneously, sand grit (aluminium oxide abrasive powder) was gradually applied on the different regions of the hull surface as shown in Fig. 2. The Wigley hull has a symmetric hull shape to the midship, therefore, the same hull surfaces can be used for both the bow-rough and aft-rough conditions by towing the model in different directions. For example, the ½-rough hull surface in Fig. 2 was used for both the ½-bow-rough and ½-aft-rough conditions as shown in Fig. 3.

A new prediction method was proposed based on the similarity law scaling (Granville, 1958, 1978) to predict the added resistance due to heterogeneous hull roughness, considering the wetted surface areas of different hull regions with different hull roughness. The similarity law scaling was performed using the roughness function, ΔU^+, of the sand grit which was obtained from our previous study (Song et al., 2020a), and the added resistance values of the Wigley model due to the heterogeneous hull roughness were predicted and compared with the results of the towing tests of the Wigley model.

2.2. Experimental setup

2.2.1. Towing tank

The towing test was carried out in the Kelvin Hydrodynamics Laboratory (KHL) of the University of Strathclyde. The tank has a dimension of 76.0 m (L) × 4.6 m (W) × 2.5 m (D). The tank is equipped with a digitally controlled towing carriage, a state-of-the-art absorbing wave maker, and a highly effective sloping beach. The carriage has a velocity range of 0–5 m/s. The carriage is able to be driven in the reverse direction. Fig. 3 shows the towing carriage in the KHL and the Wigley model towed in the forward and backward directions, with the ½-rough surface condition. Fresh water was used for the experiments, wherein the water temperature was monitored during the tests.

2.2.2. Wigley hull model

In this study, a Wigley hull model with standard proportions was used. The Wigley hull is a parabolic hull form which can be represented by

$$y = \frac{B}{2}\left[1 - \left(\frac{2x}{L}\right)^2\right]\left[1 + \left(\frac{z}{T}\right)^2\right] \tag{1}$$

where, L, B and T are the length, waterline beam and the draft of the model. The principal particulars of the Wigley model can be found in Table 1. Fig. 4 illustrates the experimental setup used for the towing test. During the test, the model was free to trim and sink. A load cell was attached at the tow point to measure the total resistance of the model
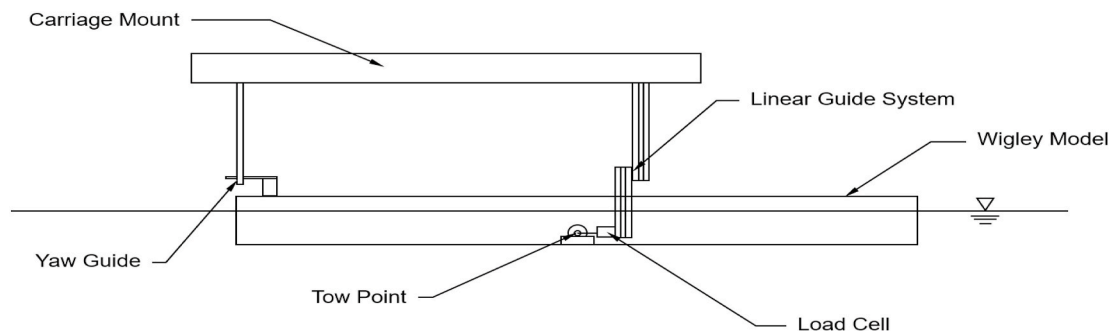

Fig. 4. Experimental set up of the towing test.

Table 2
Overall uncertainties of C_T with 95% confidence level.

Surface condition	Lowest speed		Highest speed	
	Overall Uncertainty	Percentage	Overall Uncertainty	Percentage
Smooth	±1.92E-04	±4.91%	±1.28E-04	±1.65%
¼-bow-rough	–	–	±1.25E-04	±1.44%
¼-aft-rough	±1.00E-04	±2.45%	–	–
½-bow-rough	–	–	±1.31E-04	±1.39%
½-aft-rough	±7.32E-05	±1.64%	–	–
Full-rough	±2.84E-04	±5.25%	±1.63E-04	±1.52%

ship. The model was towed with the speed range of 1.08–2.71 m/s, which corresponds to the Froude number, Fn, of 0.2–0.5. For roughening the surface, Clarke Aluminium Oxide Abrasive Powder, 60–80 grit (Rt50 = 353 μm) was applied on the surface as used by Song et al. (2020a).

2.3. Uncertainty analysis

The uncertainties of the measurements in the tests were estimated following the ITTC recommended procedures (ITTC, 2014). The precision limits were determined through the repeatability test and the bias
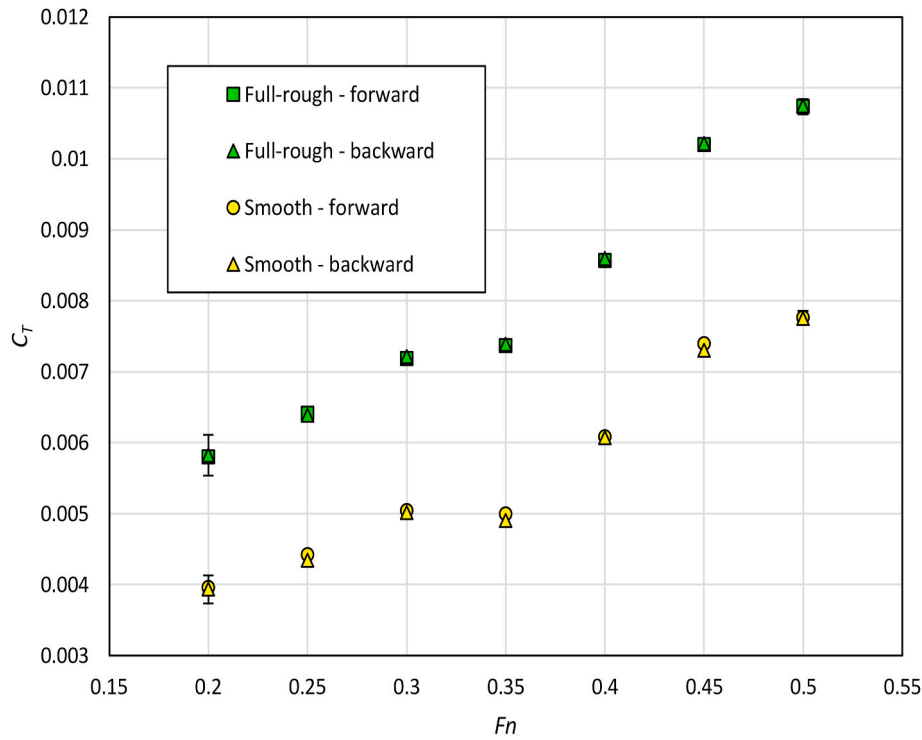

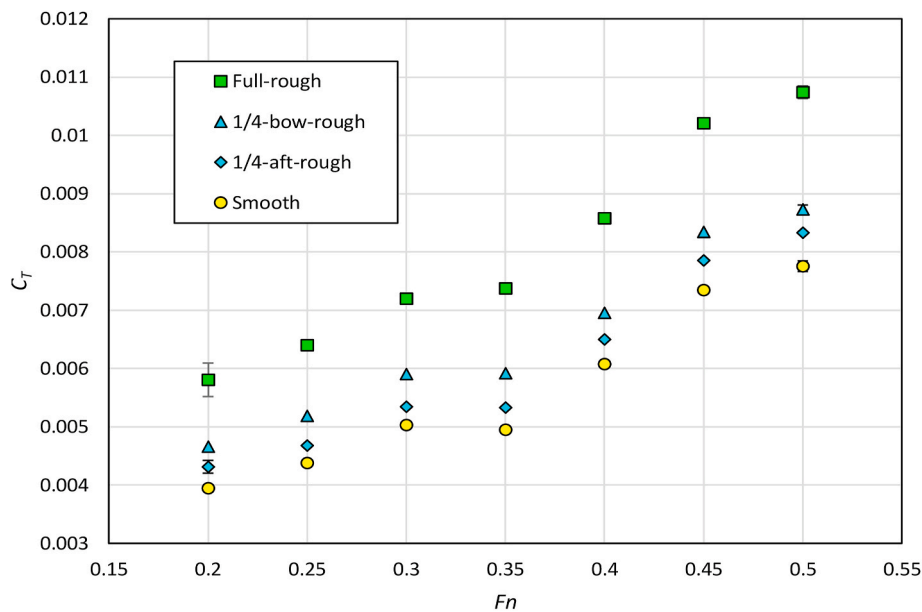**Fig. 5.** C_T values of smooth and full-rough conditions with different towing directions.

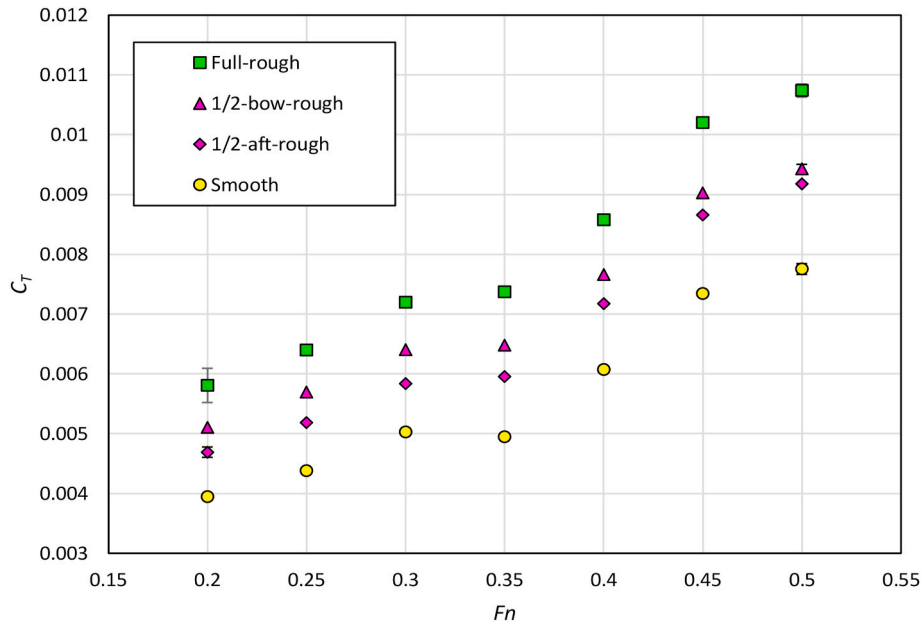**Fig. 6.** values of Wigley model in smooth and ¼-rough condition.

Fig. 7. values of Wigley model in smooth and ½-rough condition.

limits were calculated considering the uncertainties associated with the calibration, data acquisition, data reduction and conceptual bias. The repeatability tests of the bow rough conditions (e.g. ¼-bow-rough and ½-bow-rough) were conducted only at the highest speed while the repeatability tests of the aft rough conditions (e.g. ¼-aft-rough and ½-aft-rough) were conducted only at the lowest speed. Table 2 shows the absolute and relative overall uncertainties of the total resistance coefficient of the Wigley model.

3. Result

3.1. Verification of model symmetricity

As mentioned earlier, the bow-rough and aft-rough conditions (e.g. ½-bow-rough and ½-aft-rough in Fig. 1) were realised by towing the model in different directions while using the same hull surfaces (e.g. ½-rough surface in Fig. 2) as shown in Fig. 3. Therefore, it is necessary to verify the model symmetricity before investigating the effect of heterogeneous hull roughness. The towing test results of the homogeneous

hull conditions (e.g. smooth and full-rough conditions) in different towing directions were compared for the verification of the model symmetricity.

Fig. 5 compares total resistance coefficient, C_T, of the Wigley model with the homogeneous hull conditions (e.g. smooth and full-rough conditions). As shown in the figures, the C_T values of the smooth condition were observed not to be significaltly affected by the towing directions, showing the deviations within the uncertainty levels of the experiment. This suggests that the geometric accuracy of the model is within a satisfactory level. Therefore, the differences between the bow and aft rough conditions (i.e. difference between ¼-bow-rough and ¼-aft-rough conditions) can be purely attributed to the different locations of the hull roughness. Similarly, the C_T values of the full-rough conditions were almost identical regardless of the towing directions. This validates again the geometric symmetricity of the model and also suggests that the potential imperfections of the sand grit application do not affect the result significantly.
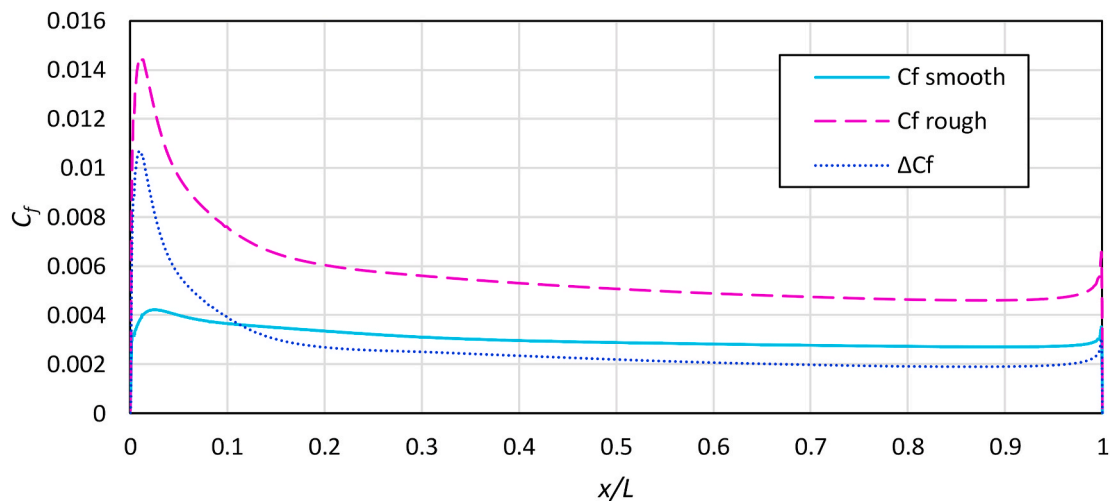

Fig. 8. Local skin friction on the flat plate along the line of $z = -2/T$ in smooth and (homogeneously) rough condition with the towing speed of $V = 4.5 \, m/s$, obtained from the CFD simulation of Song et al. (2020e).
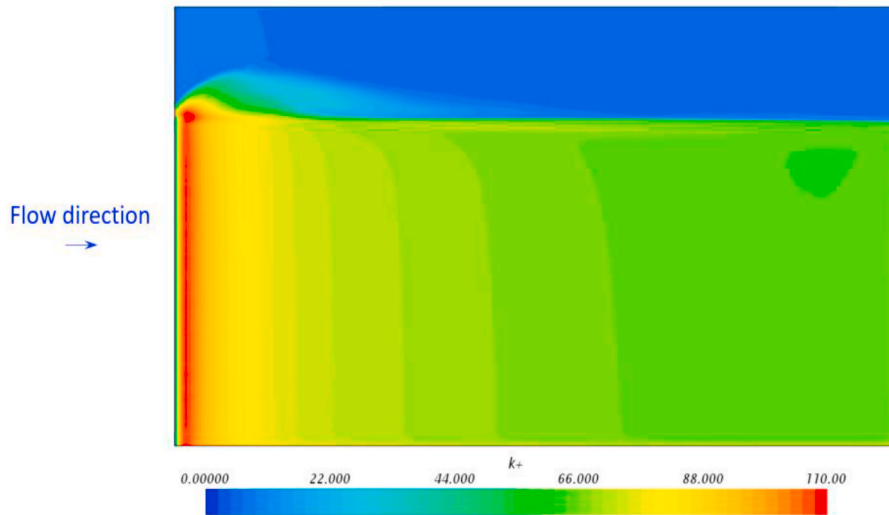
Fig. 9. Roughness Reynolds number, k^+, on the rough flat plate with the towing speed of $V = 4.5 \, m/s$, obtained from the CFD simulation of Song et al. (2020e).

3.2. Effect of heterogeneous hull roughness

As shown in Fig. 6, the model with the ¼-bow-rough condition showed larger C_T values compared to the C_T values of the ¼-aft-rough condition. The percentage increases in C_T compared to the smooth condition, %ΔC_T, are 12–18% for the ¼-bow-rough condition, and 8–10% for the ¼-aft-rough condition. Similarly, the Wigley hull with the ½-bow-rough condition showed larger C_T values than the results of the ½-aft-rough condition as shown in Fig. 7. The %ΔC_T values with the ½-bow-rough condition are 21–30%, while these values are 16–22% for the ½-aft-rough condition.

These results imply that the hull roughness of the fore part of the ship results in greater added resistance than the roughness of the aft part.

3.3. Rationale behind the effect of heterogeneous roughness

As differences in the roughness effect on the C_T were observed between the bow-rough and aft-rough conditions as shown in Figs. 6 and 7, it is worthwhile to discuss the possible rationale behind this observation. One of the most likely reason is the varying contributions of the local skin friction, C_f, to the total drag of the ship. It is a well-known fact that, regardless of the roughness effect, the C_f is larger near the leading edge due to the active transition behaviours and it decreases as the flow is developed along the hull (i.e. the bow region of the Wigley model has larger wall shear stress, τ_w). Accordingly, the roughness Reynolds numbers, $k^+ = kU_\tau/\nu$, in the bow region become larger and the roughness effect in this region becomes more evident, where k is the roughness height, $U_\tau = \sqrt{\tau_w/\rho}$ is the frictional velocity and ν is the kinematic viscosity of water.

Although the local skin friction on the Wigley model was not measured during the test, alternatively, this rationale could be supported by CFD simulations conducted in our previous study which involves a 1.5 m towed flat plate in smooth and rough surface conditions (Song et al., 2020e). Fig. 8 compares the C_f values of the plate in the smooth and rough conditions along the line of $z = -2/T$, and the difference, ΔC_f, between the smooth and rough cases.

As shown in the figure, the smooth plate shows larger C_f near the leading edge and the values gradually reduce along the flat plate. The rough plate shows an even larger peak of the C_f near the leading edge. Accordingly, the ΔC_f is greater in the forward region and it reduces gradually along the plate, which is in correspondence with the k^+ values on the plate surface as shown in Fig. 9. It is of note that Fig. 9 shows the k^+ values on the vertically towed flat plate crossing free surface, and

therefore low k^+ values appear in the dry region above the free surface due to the low viscosity of air.

From this observation, it can be deduced that the roughness effect on the skin friction (i.e. ΔC_f) is greater in the forward region of the flat plate and the same logic can be applied to ship hulls.

4. New prediction method for heterogeneous hull roughness

In this study, a new prediction method was developed for the added resistance of a ship due to the heterogeneous hull roughness, based on the added resistance predictions obtained from the similarity law scaling of Granville (1958; 1978). This new method considers the effect of different wetted surface areas of the individual regions with different hull roughness, while neglecting the effect of the different locations of the roughness.

The added frictional resistance of a ship, ΔC_F, with N different roughness regions is determined as

$$\Delta C_F = \sum_{i=1}^{N} \frac{WSA_i}{WSA_{ship}} \Delta C_{F,i} \qquad (2)$$

where, WSA_i is the wetted surface area of the ith region, WSA_{ship} is the total wetted surface area of the ship. $\Delta C_{F,i}$ is the added frictional resistance with the hull roughness in the ith region obtained from the Granville's method, under the assumption of the homogeneous distribution of the given hull roughness. Details of Granville's similarity law scaling can be found in our previous studies (Demirel et al., 2019; Song et al., 2020a).

The frictional resistance of the ship $C_{F,r}$ with heterogeneous hull roughness can be determined as

$$C_{F,r} = C_{F,s} + \Delta C_F \qquad (3)$$

in which, $C_{F,s}$ is the frictional resistance coefficient of a smooth ship that can be obtained by using Kàrmàn-Schoenherr friction line (Schoenherr, 1932), as

$$\frac{0.242}{\sqrt{C_F}} = \log(Re_L C_F) \qquad (4)$$

where, Re_L is the Reynolds number based on the length of the ship.

The obtained $C_{F,r}$ can be used to predict the total resistance coefficient, C_T, of a ship with heterogeneous hull roughness. Recently, Song et al. (2020a) used two different added resistance prediction methods due to hull roughness, based on the hypotheses of Froude and Hughes,
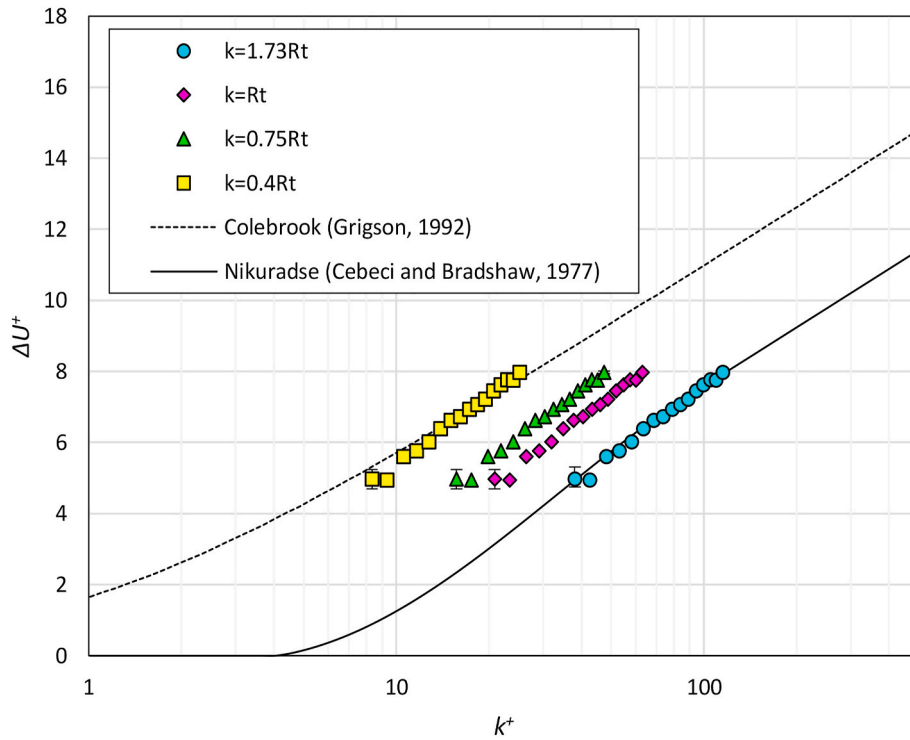
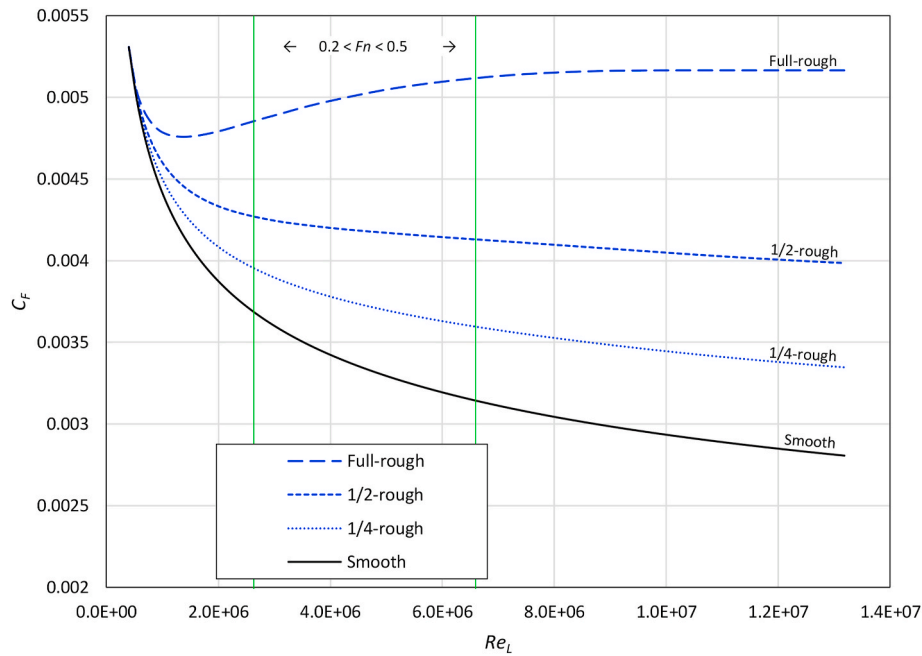**Fig. 10.** Roughness functions of the sand grit surface, adapted from Song et al. (2020a) (Grigson, 1992).

Fig. 11. C_F predictions of the Wigley hull with different surface conditions.

namely *2D method* and *3D method*. Song et al. (2020a) concluded that the *3D method* predicts the total resistance more accurately than the *2D method*, due to the fact that the hull roughness not only affects the skin friction but also increases the viscous pressure resistance, C_{VP}. This conclusion is supported by other recent studies involving CFD simulations (Song et al., 2019a, 2020c, 2020d). Therefore, *3D method* is used to predict the C_T of the Wigley model together with the obtained $C_{F,r}$ values.

In the *3D method*, the total resistance for the rough ship model, $C_{T,r}$, is determined by

$$C_{T,r} = (1+k)C_{F,r} + C_W \tag{5}$$

where, C_W is the wave-making resistance of the ship. k is the form factor of the ship.

4.1. Resistance prediction and comparison against EFD

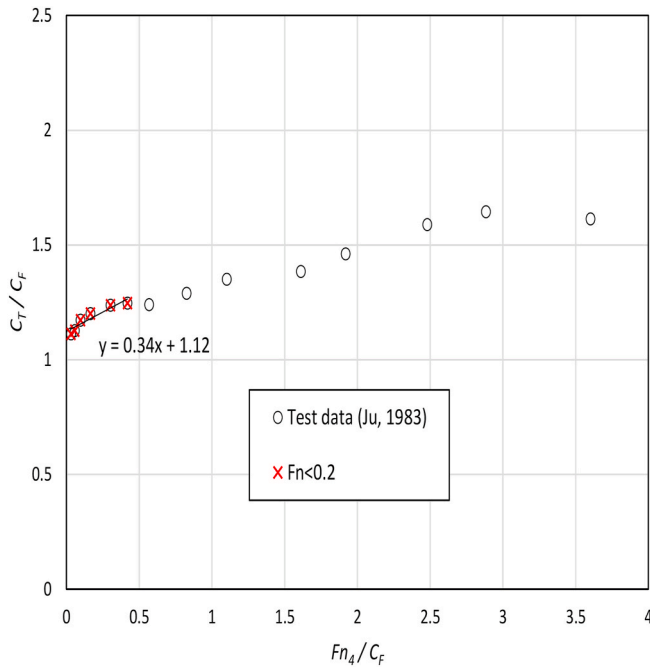Before predicting the frictional resistance of the Wigley model with

Fig. 12. Form factor calculation based on the test data of Ju (1983).

$$\Delta U^+ = \begin{cases} 0 & \rightarrow \quad k^+ < 2.25 \\ \frac{1}{\kappa}\ln(0.253k^+)^{\sin\left[\frac{\pi}{2}\frac{\log(k^+/2.25)}{\log(90/2.25)}\right]} & \rightarrow \quad 2.25 \le k^+ < 90 \\ \frac{1}{\kappa}\ln(0.253k^+) & \rightarrow \quad 90 \le k^+ \end{cases} \quad (6)$$

Fig. 11 shows the C_F values of the Wigley hull with different surface conditions, predicted using the newly proposed method (Equations (2) and (3)). In the figure, the smooth type C_F values were calculated using the Kàrmàn-Schoenherr friction line (Equation (4)).

To calculate the C_T of the ship using the *3D method*, the form factor, k, and the wave-making resistance coefficient, C_W, values are needed (Equation (5)). Unfortunately, the Prohaska's test could not be conducted in this study, as the result at low towing speed ($Fn < 0.2$) was unstable due to the absence of turbulence stimulator. Alternatively, the form factor was obtained by reproducing the experimental data of Ju (1983), which used a similar length ($L=3.048$ m) of Wigley model with a similar water temperature (13 °C) as well as the same free trim and sinkage condition. As shown in Fig. 12, the form factor value ($k=0.12$) was calculated using a regression line of the data at the low speed region ($Fn < 0.2$). Also, the potential-based C_W values for the Wigley hull with free trim and sinkage, determined by Chen et al. (2019), were used for the C_T prediction.

Figs. 13–15 show the C_T of the Wigley model obtained from the towing test and the predicted C_T values from the newly proposed method. The predicted C_T values show a reasonable agreement with the towing test results. As shown in Figs. 13 and 14, the predicted C_T values of the heterogeneous hull conditions located mostly in between the bow-rough and aft-rough results of the experiment. This can be attributed to the fact that the newly proposed prediction method does not consider the effect of different locations of the hull roughness, while it considers the effect of the different wetted surface areas of the individual roughness regions. On the other hand, the prediction for the full-rough condition shows a fair agreement in general as shown in Fig. 15, but relatively higher deviations were observed at high speeds ($Fn \ge 0.4$). Possible reasons for these deviations include the unknown impacts of hull roughness on the form factor k and wave making resistance, C_W,

different surface conditions using Equation (2), the frictional resistance of the sand grit surface was predicted first using the similarity law scaling. Song et al. (2020a) showed that the roughness functions of the same sand grit surface follow the Nikuradse-type roughness function model of Cebeci and Bradshaw (1977) when the equivalent sand-grain roughness height, $k_s = 1.73Rt_{50}$, is used ($Rt_{50}=353$ μm), as shown in Fig. 10.

Therefore, the similarity law scaling was conducted using the roughness function model of Cebeci and Bradshaw (1977), defined as,
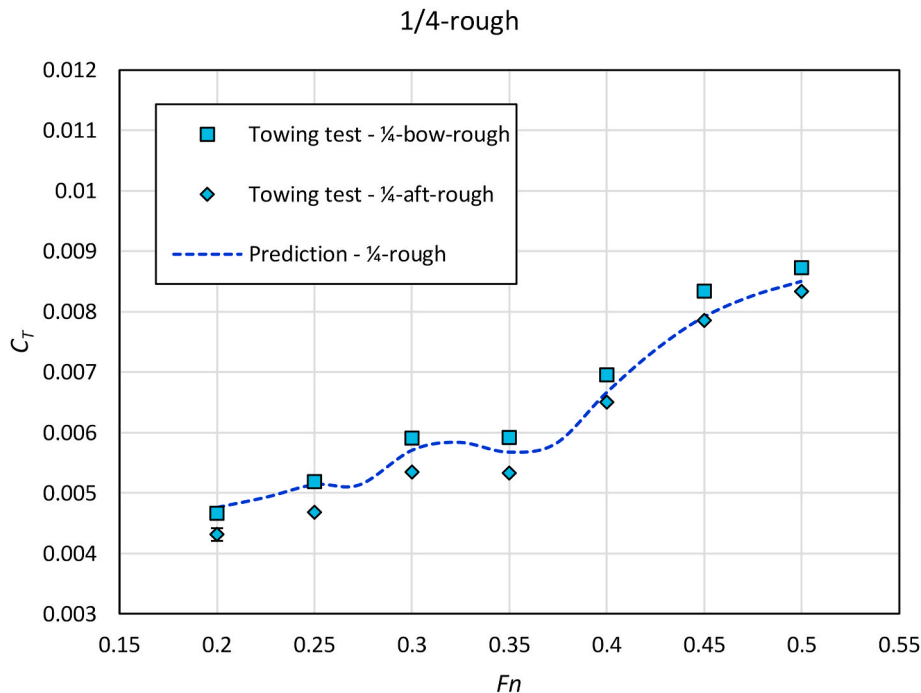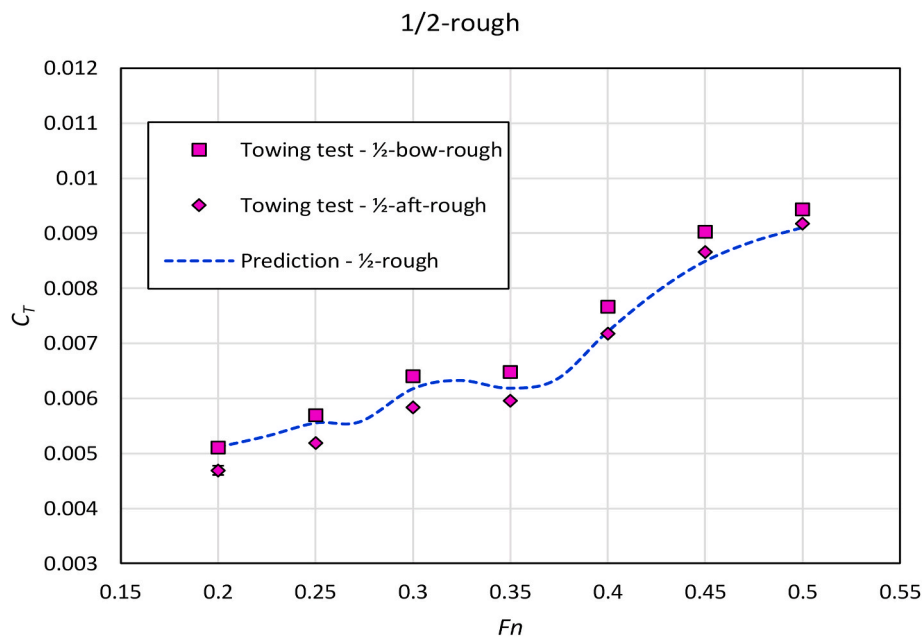

Fig. 13. values from the towing test and the predictions for the Wigley model with ¼-rough condition.

1/2-rough

Fig. 14. values from the towing test and the predictions for the Wigley model with ½-rough condition.
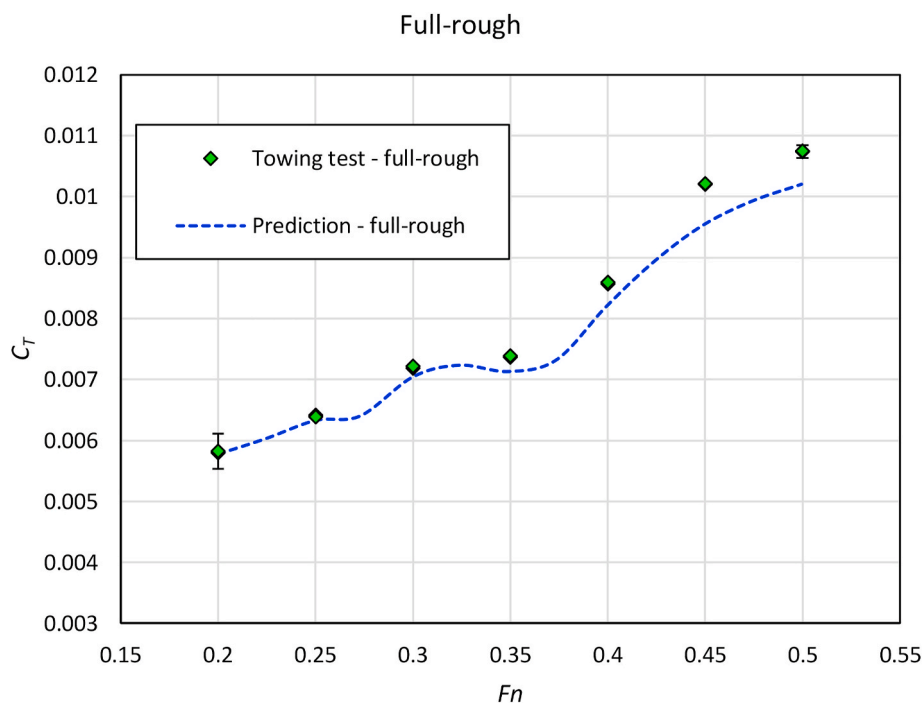
Full-rough

Fig. 15. values from the towing test and the predictions for the Wigley model with full-rough condition.

inaccuracies of the Granville's extrapolation as well as the uncertainties of the experimentally obtained roughness functions. It is of note that this new prediction method does not differ from the conventional Granville's approach for a homogeneously distributed hull roughness (e.g. full-rough condition in Fig. 15).

5. Concluding remarks

Towing tests were conducted involving a Wigley hull model with different hull roughness conditions, including the heterogeneous hull conditions (i.e. ¼-bow-rough, ¼-aft-rough, ½-bow-rough and ½-aft-rough conditions) and the homogeneous hull conditions (i.e. smooth and full-rough conditions). The bow-rough conditions (i.e. ¼-bow-rough and ½-bow-rough) showed larger added resistance compared to the aft-rough conditions (¼-aft-rough and ½-aft-rough) with the same wetted surface area of the roughness region. The finding suggests that the hull roughness of the front part of the ship results in more added resistance than the hull roughness in other regions. The rationale behind this difference was discussed with an example of a CFD simulation conducted in the previous study (Song et al., 2020e).

A new method was proposed to predict the effect of heterogeneous hull roughness on ship resistance, based on the similarity law scaling. The method considers the different wetted surface areas of the different roughness regions, while neglecting the location of the hull roughness.

The results predicted using the newly proposed method showed a reasonable agreement with the towing test results. Considering that the heterogeneous roughness conditions used in this study are rather extreme (i.e. sudden changes in the hull roughness from a smooth surface to a remarkably rough surface), the newly proposed method could establish better predictions for real ship cases with milder heterogeneous distributions of hull roughness. Therefore, future work may include applying the new prediction method for other types of hull conditions such as heterogeneous fouling surfaces.

The study presents a useful investigation into the effect of heterogeneous hull roughness, suggesting that the hull roughness in different locations can bring different roughness effects on the ship resistance. For better understandings regarding this new observation, the study should be extended using CFD simulations, which will enable an investigation into the flow characteristics around the heterogeneous hull roughness. Another recommended future work is case studies to predict the added resistance due to heterogeneous hull roughness using CFD simulations and the newly proposed prediction method, to examine the agreement between these low and high-fidelity methods.

CRediT authorship contribution statement

Soonseok Song: Writing - original draft, Data curation, Software, Formal analysis, Investigation, Validation, Visualization. **Roberto Ravenna:** Data curation, Investigation, Formal analysis. **Saishuai Dai:** Data curation, Investigation, Validation. **Claire DeMarco Muscat-Fenech:** Writing - review & editing, Project administration, Funding acquisition. **Giorgio Tani:** Writing - review & editing, Project administration, Supervision. **Yigit Kemal Demirel:** Conceptualization, Methodology, Supervision, Writing - review & editing, Project administration, Resources, Funding acquisition. **Mehmet Atlar:** Writing - review & editing, Project administration, Supervision. **Sandy Day:** Resources, Writing - review & editing, Project administration, Supervision.

Declaration of competing interest

The authors declare that they have no known competing financial interests or personal relationships that could have appeared to influence the work reported in this paper.

Acknowledgement

References

Cebeci, T., Bradshaw, P., 1977. Momentum Transfer in Boundary Layer, Vol. –1.

Chen, X., Zhu, R.-c., Song, Y.-l., Fan, J., 2019. An investigation on HOBEM in evaluating ship wave of high speed displacement ship. J. Hydrodyn. 31 (3), 531–541. https://doi.org/10.1007/s42241-018-0092-8.

Demirel, Y.K., Khorasanchi, M., Turan, O., Incecik, A., Schultz, M.P., 2014. A CFD model for the frictional resistance prediction of antifouling coatings. Ocean Eng. 89, 21–31. https://doi.org/10.1016/j.oceaneng.2014.07.017.

Demirel, Y.K., Song, S., Turan, O., Incecik, A., 2019. Practical added resistance diagrams to predict fouling impact on ship performance. Ocean Eng. 186, 106112 https://doi.org/10.1016/j.oceaneng.2019.106112.

Demirel, Y.K., Turan, O., Incecik, A., 2017a. Predicting the effect of biofouling on ship resistance using CFD. Appl. Ocean Res. 62, 100–118. https://doi.org/10.1016/j.apor.2016.12.003.

Demirel, Y.K., Uzun, D., Zhang, Y., Fang, H.-C., Day, A.H., Turan, O., 2017b. Effect of barnacle fouling on ship resistance and powering. Biofouling 33 (10), 819–834. https://doi.org/10.1080/08927014.2017.1373279.

Farkas, A., Degiuli, N., Martić, I., 2018. Towards the prediction of the effect of biofilm on the ship resistance using CFD. Ocean Eng. 167, 169–186. https://doi.org/10.1016/j.oceaneng.2018.08.055.

Farkas, A., Song, S., Degiuli, N., Martić, I., Demirel, Y.K., 2020. Impact of biofilm on the ship propulsion characteristics and the speed reduction. Ocean Eng. 199, 107033 https://doi.org/10.1016/j.oceaneng.2020.107033.

Flack, K.A., Schultz, M.P., 2010. Review of hydraulic roughness scales in the fully rough regime. J. Fluid Eng. 132 (4), 41203–41210. https://doi.org/10.1115/1.4001492.

Granville, P.S., 1958. The frictional resistance and turbulent boundary layer of rough surfaces. J. Ship Res. 2 (3), 52–74.

Granville, P.S., 1978. Similarity-law Characterization Methods for Arbitrary Hydrodynamic Roughnesses (Bethesda, MD).

Grigson, C., 1992. Drag losses of new ships caused by hull finish. J. Ship Res. 36, 182–196.

Li, C., Atlar, M., Haroutunian, M., Norman, R., Anderson, C., 2019. An investigation into the effects of marine biofilm on the roughness and drag characteristics of surfaces coated with different sized cuprous oxide (Cu2O) particles. Biofouling 1–19. https://doi.org/10.1080/08927014.2018.1559305.

Pullin, D.I., Hutchins, N., Chung, D., 2017. Turbulent flow over a long flat plate with uniform roughness. Physical Review Fluids 2 (8), 82601. https://doi.org/10.1103/PhysRevFluids.2.082601.

Schoenherr, K.E., 1932. Resistance of flat surfaces moving through a fluid. Trans SNAME 40, 279–313.

Schultz, M.P., 2002. The relationship between frictional resistance and roughness for surfaces smoothed by sanding. J. Fluid Eng. 124 (2), 492–499. https://doi.org/10.1115/1.1459073.

Schultz, M.P., 2004. Frictional resistance of antifouling coating systems. J. Fluid Eng. 126 (6), 1039–1047. https://doi.org/10.1115/1.1845552.

Schultz, M.P., Bendick, J.A., Holm, E.R., Hertel, W.M., 2011. Economic impact of biofouling on a naval surface ship. Biofouling 27 (1), 87–98. https://doi.org/10.1080/08927014.2010.542809.

Schultz, M.P., Flack, K.A., 2007. The rough-wall turbulent boundary layer from the hydraulically smooth to the fully rough regime. J. Fluid Mech. 580, 381–405. https://doi.org/10.1017/S0022112007005502.

Song, S., Dai, S., Demirel, Y.K., Atlar, M., Day, S., Turan, O., 2020a. Experimental and theoretical study of the effect of hull roughness on ship resistance. J. Ship Res. https://doi.org/10.5957/JOSR.07190040 (Preprint).

Song, S., Demirel, Y.K., Atlar, M., 2019a. An Investigation into the Effect of Biofouling on Full-Scale Propeller Performance Using CFD. https://doi.org/10.1115/OMAE2019-95315.

Song, S., Demirel, Y.K., Atlar, M., 2019b. An investigation into the effect of biofouling on the ship hydrodynamic characteristics using CFD. Ocean Eng. 175, 122–137. https://doi.org/10.1016/j.oceaneng.2019.01.056.

Song, S., Demirel, Y.K., Atlar, M., 2020b. Penalty of hull and propeller fouling on ship self-propulsion performance. Appl. Ocean Res. 94, 102006 https://doi.org/10.1016/j.apor.2019.102006.

Song, S., Demirel, Y.K., De Marco Muscat-Fenech, C., Tezdogan, T., Atlar, M., 2020c. Fouling effect on the resistance of different ship types. Ocean Eng. 216, 107736 https://doi.org/10.1016/j.oceaneng.2020.107736.

Song, S., Demirel, Y.K., Atlar, M., Shi, W., 2020d. Prediction of the fouling penalty on the tidal turbine performance and development of its mitigation measures. Appl. Energy 276, 115498. https://doi.org/10.1016/j.apenergy.2020.115498.

Song, S., Demirel, Y.K., Atlar, M., Dai, S., Day, S., Turan, O., 2020e. Validation of the CFD approach for modelling roughness effect on ship resistance. Ocean Eng. 200, 107029 https://doi.org/10.1016/j.oceaneng.2020.107029.

Tezdogan, T., Demirel, Y.K., 2014. An overview of marine corrosion protection with a focus on cathodic protection and coatings. Brodogradnja 65, 49–59.

Townsin, R.L., 2003. The ship hull fouling penalty. Biofouling 19 (1), 9–15. https://doi.org/10.1080/0892701031000088535.

Uzun, D., Demirel, Y.K., Coraddu, A., Turan, O., 2019. Time-dependent biofouling growth model for predicting the effects of biofouling on ship resistance and powering. Ocean Eng. 191, 106432 https://doi.org/10.1016/j.oceaneng.2019.106432.

Uzun, D., Ozyurt, R., Demirel, Y.K., Turan, O., 2020. Does the barnacle settlement pattern affect ship resistance and powering? Appl. Ocean Res. 95, 102020 https://doi.org/10.1016/j.apor.2019.102020.